IEICE Electronics Express, Vol.17, No.1, 1–5

LETTER

A wideband transmitarray using triple-layer elements with reduced profile

Xiuzhu Lv[1], Zhihua Han[1], Xin Jian[1], Yongliang Zhang[1,2a)], and Qiang Chen[3]

Abstract A triple-layer wideband transmitarray (TA) which works at 18.5 GHz with reduced profile is presented in this paper. The unit cell composed of three metal layers, each layer is etched on the corresponding dielectric substrate. The top layer consists of double square rings, the same as the bottom layer. The intermediate layer consists of a Jerusalem cross slot. The thickness of designed unit cell is 0.15λ, where λ is the wavelength in free-space. A large frequency range is implemented by parallel sets of phase curves generated by proposed unit cell. The magnitude of transmission coefficient is less than 1 dB and the phase shift range exceeds 360 degree across the entire frequency range. We design, fabricate and measure a TA operating at 18.5 GHz to show the validation of this paper. Through the measurement, we can obtain that the 1-dB gain bandwidth is 14.8% (17.5–20.3 GHz), and maximum gain is 22.5 dB at 18.5 GHz. The proposed transmitarray's maximum aperture efficiency is 46%.

Keywords: wideband, reduced profile, transmitarray antenna, triple-layer
Classification: Microwave and millimeter-wave devices, circuits, and modules

1. Introduction

The transmitarray (TA) antenna combines the advantages of the parabolic antenna such as high gain, high radiation efficiency, light-weight [1]. Thus, it has high potential to be applied in a wide range of wireless communication systems. A typical TA consists of an feed horn and multiple layers of flat transmitting surfaces, which have a 2-D array of transmission unit cells [2], as shown in Fig. 1. By tuning the transmission phase of each unit cell, the transmitting phase can be compensated, and the spherical wave emitted by the feed source can be converted into plane wave. As a consequence, the TA can form a focused beam with high gain. Because the TA size contains multiple wavelengths, the distance from the feed horn to the unit cell is much larger than several wavelengths according to the focal diameter ratio. Therefore, the TA unit cell should have phase shift greater than 360°. Despite the aforementioned advantages, the transmitarray has the defect of limited bandwidth, which is typically about 5% or less.

[1]College of Electronic Information, Engineering Inner Mongolia University, Hohhot 010021, China
[2]College of Transportation, Inner Mongolia University, Hohhot 010021, China
[3]Department of Communications Engineering Graduate, School of Engineering, Tohoku University, 6–6–05 Aoba-yama, Sendai 980–8579, Japan
a) namar@imu.edu.cn

DOI: 10.1587/elex.16.20190678
Received November 11, 2019
Accepted November 22, 2019
Publicized December 13, 2019
Copyedited January 10, 2020

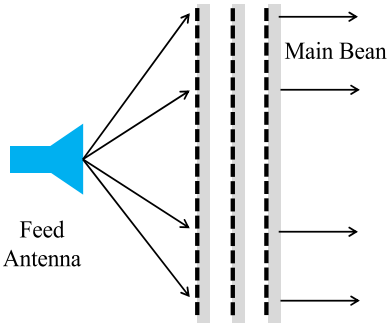

Fig. 1. Geometry of the triple-layer transmitarray antenna.

Many researchers have made efforts to improve the bandwidth performance of TA antennas. Using multilayer frequency-selective surface unit cells is a typical approach [1, 2, 3, 4, 5, 6, 7, 8, 9, 10, 11, 12]. In [1], a four-layer TA without dielectric substrate by using cross-slot unit cells is presented. However, as the angle of oblique incidence increases, the transmission coefficient of the unit cell becomes worse, which leads to the gain degradation. In [2], a four-layer TA using double split ring slot is presented, the total thickness of the proposed antenna is 0.75λ. Split diagonal cross unit cells based triple-layer transmitarray can realize a maximum gain of 18.9 dB, and 1-dB bandwidth is 9.6% [3]. In [4], rectangle ring slot unit cells based multiple-polarization transmitarray is reported. 1-dB gain bandwidth of 8.3% and maximum gain of 20.1 dB are achieved. The authors in [5] demonstrate a four-layer TA which is implemented by dual-resonant double square ring. The measured results show that transmitarray 7.5% 1-dB bandwidth and 47% aperture efficiency can be achieved. The TA design in [6] provides 9% 1-dB bandwidth with a thickness of 0.51λ. In [7], the TA achieves 16% 1-dB gain bandwidth with a thickness of 0.36λ. However, the TA unit cell consists six layers of patches, which would increase fabricate cost. In [13, 14, 15, 16, 17], delay lines are used to enlarge the range of the phase shift, and freedom of the design parameters are added. In [18], a novel TA based novel ultrathin slot is reported. The 1-dB gain bandwidth and efficiency are 5.7% and 38% at the center frequency, respectively. TAs are constructed using metal and dielectric materials to improve bandwidth in [20, 21, 22]. Wideband array antennas design based on digital coding are proposed in [23, 24, 25]. Other researches on reconfigurable antenna are reported in [26, 27, 28, 29, 30].

Bandwidth limitation and antenna thickness are two limitations for antenna arrays. In order to rectify these two

limitations, a novel triple-layer transmitarry operating at 18.5 GHz is presented in this paper. Because of the novel composition method, the proposed TA unit achieves phase shift of more than 360 degrees and has low transmission loss. Using the proposed unit cell, we present a TA consisting of 15×15 unit cells. The measured result agree with the simulated result well. The proposed design provides a cost-effective method to realizing wideband, reduced profile and high efficiency transmitarrays.

The structure of this paper is as follows. Introduction is given in Section I. The TA unit cell proposed in this paper is designed and analyzed in Section II. In order to better demonstrate the working principle, we perform the parametric analysis of the TA unit cell. Then, a TA antenna prototype is fabricated and the measured results are presented and discussed in Section III. Finally, the conclusion is drawn in the Section IV.

2. Design of the TA unit cell

2.1 TA unit cell structure

As shown in Fig. 2, the transmitarray unit cell composed of three metal layers, each layer is etched on the corresponding dielectric substrate. The top layer consists of double square rings which is shown in Fig. 2(a), the same as the bottom layer. The intermediate layer consists of a Jerusalem cross slot which is shown in Fig. 2(b). The dielectric substrate thickness is 0.5 mm, the relative dielectric constant is 2.2, and the loss tangent is 0.001. The dielectric substrates apart from each other by same air gaps (H1) in between.

Four-layers unit cell with double square rings is used in [5] to cover a full transmission phase range. In order to achieve low profile characteristics while maintaining wideband performance, we use a Jerusalem cross slot in the intermediate layer, which is shown in Fig. 2(b). Ordinary three-layer double-ring structure can only form one resonance point. The addition of different intermediate layer can form two resonance points, which are the resonance between the upper and lower layers and the resonance between the upper and lower layers and intermediate layer, respectively. Fig. 3 is the resonance characteristic of the unit cell, as shown in the figure, the unit cell has two resonance points. Therefore, the unit cell could cover sufficient phase range. By adjusting the size of the unit cell, the resonant point of the unit cell is adjusted to make the resonant point approach each other, so that a large transmission response could be realized. The TA unit cell is simulated and optimized by commercial soft-ware Ansys HFSS. To analyze the properties of the unit cell, master-slave boundary bars are used to simulate the surface of a planar periodic structure. In order to get the desired phase shift curve, the parameters of the TA unit cell must be adjusted during the design process. Table I shows the specific dimensions of the unit cell.

Fig. 4 shows the variation of transmission amplitude and phase with parameter S at 18.5 GHz. The transmission phase range exceeds 360 degree, and the transmission loss is less than 1 dB. When S varies from 2 mm to 4.5 mm, the phase shift of the TA unit cell at different frequency is shown in Fig. 5. From Fig. 5, we can see that the transmission phase curves are parallel within the 3 GHz frequency range. A wideband response can be implemented by this TA unit cell.

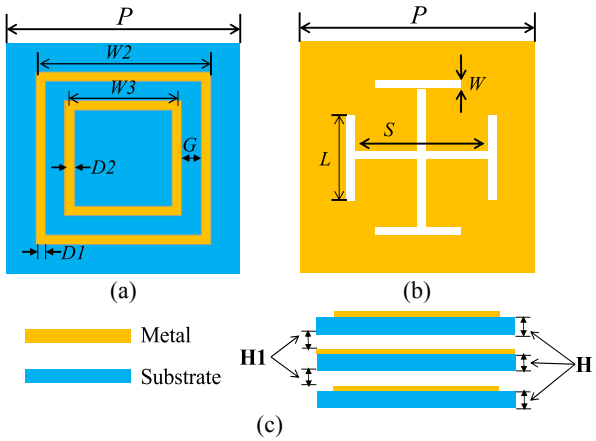

Fig. 2. Configuration of the TA unit cell. (a) Double square ring (on the top and bottom layers). (b) Jerusalem cross slot (on the intermediate layer). (c) The triple-layer TA unit cell.

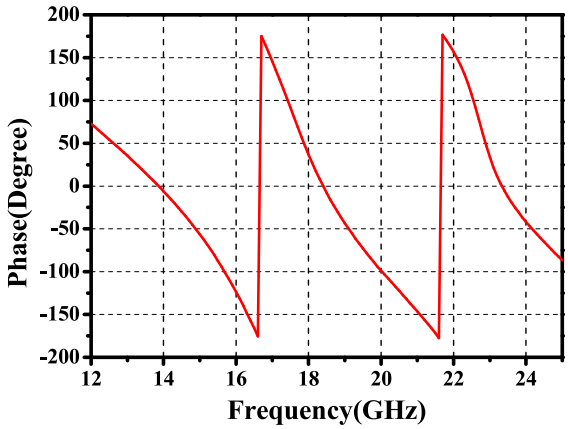

Fig. 3. Resonance characteristics of TA unit cell when S is 2.8 mm.

Table I. Design parameters of the TA unit cell

Parameter	Value
P	6 mm
$D1$	0.2 mm
$D2$	0.2 mm
L	1.8 mm
W	0.18 mm
$W2$	$1.2 * S$
$W3$	$W2 - 2 * D1 - 2 * G$
G	0.5 mm
H	0.5 mm
H1	0.5 mm
S	Vary

2.2 Oblique incidence conditions

When the transmitarray is illuminated by a feed horn, the electric field from the feed incidenting all unit cells is not uniform, the incidence angle of most unit cells is oblique. The transmitarray bandwidth is influenced by oblique in-

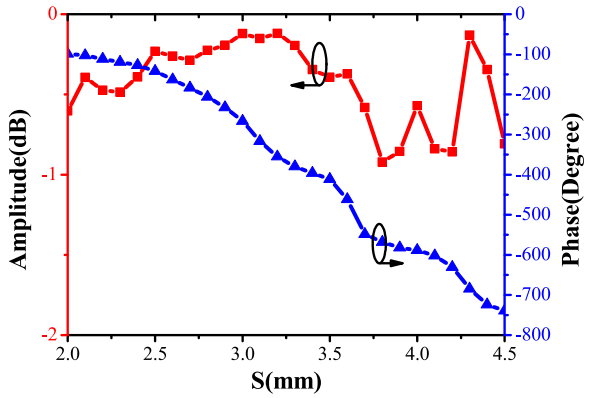

Fig. 4. Simulated transmission amplitude and phase.

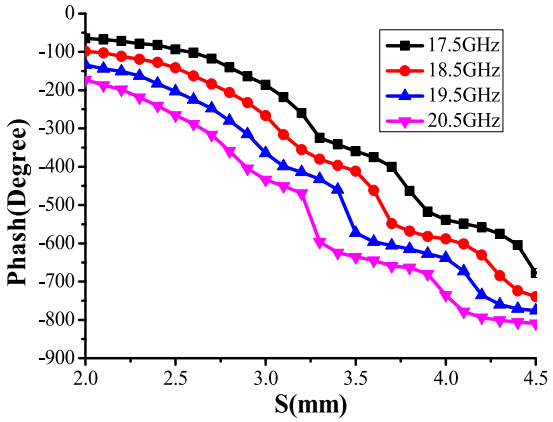

Fig. 5. Transmission phases versus S for different frequencies.

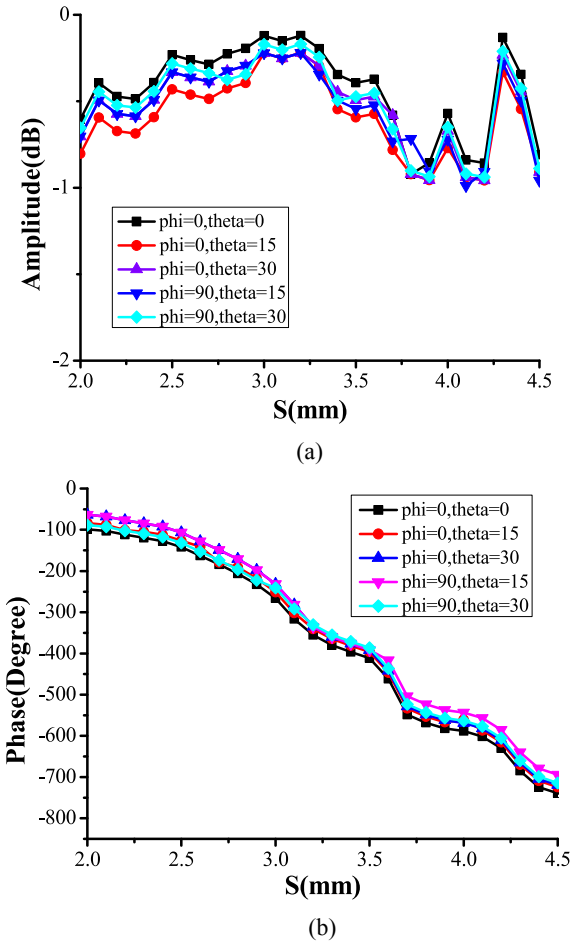

Fig. 6. Transmission coefficient versus S at different oblique incidence angles. (a) Amplitude. (b) Phase.

cidence performance of the unit cell greatly. Therefore, we need to consider the influence of different incident angles on the unit cell performance. θ and φ are the angles between the incident direction and the Z and X axis, respectively. Fig. 6 shows the transmission coefficient amplitude and phase curves at different oblique incidence angles. The maximum deviation of phase shift at different incident angles is 50 degrees, which has little influence on the overall design of the array and is acceptable. From Fig. 6, it can be seen that TA unit cell has relatively low transmission loss and is less affected by oblique incident electromagnetic wave. Thus, the designed unit cell can be used to construct transmitarry antenna.

3. Transmitarray design and measurements

3.1 Design of transmitarray antenna

In order to form a better main beam pattern in expected direction, the TA unit cell needs to compensate for the phase difference of spatial delay caused by different propagation paths, which is also a crucial step in the design and research of the transmitarray antenna. Reasonable and accurate phase compensation can obtain the expected gain curve and the ideal beam direction pattern.

The phase compensation of each unit cell φ_i according to the unit cell position (x_i, y_i) in the array, the feed location (x_f, y_f), and the generated beam direction (θ_0, φ_0) as follows:

$$\varphi_i(x_i, y_i) = k_0(d_i - sin\theta_0(x_i cos\varphi_0 + y_i sin\varphi_0)) \quad (1)$$

where k_0 is the propagation constants in vacuum, and the distance from the feed to the i-th unit cell is di

$$d_i = \sqrt{(x_i - x_f)^2 + (y_i - y_f)^2 + {z_f}^2} \quad (2)$$

It can be seen from Eq. (1) that the phase compensation value required by the unit cell is related to the position of the feed, the angle of incidence, the position of the unit cell and the propagation constant. In the design of transmitarray antenna, the distribution of the aperture field is determined after the position of the feed is given, so the phase compensation value of each element is determined by the location of the element. By changing the size of the element, the phase can be compensated.

Based on the above theoretical basis, a 255-unit cell TA using the proposed unit cell is designed, fabricated, and measured to show the validation of the proposed wideband TA unit cell. The dimension of the TA is 90 mm × 90 mm × 2.5 mm, and the corresponding thickness is 0.15λ. Consider the effect of the edge illumination levels on the aperture efficiency and sidelobe levels, a wideband pyramidal horn is chosen as the feed antenna. The aperture size of the horn is 69 mm ∗ 55 mm, and the gain of the horn is 18.9 dB at 18.5 GHz. F is the focal distance, and the value is 90 mm. (F/D) is the focal length to diameter ratio, and the value is 1. By using Eq. (1), we can calculate the transmission phase of each unit cell in the transmitarray, which is shown in Fig. 7. Once we obtain the transmission phase of i-th

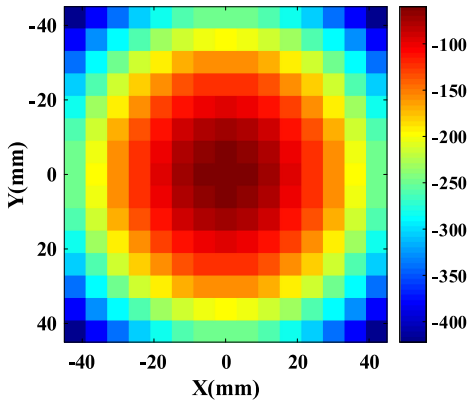

Fig. 7. Transmission phase distribution of transmitarray antenna.

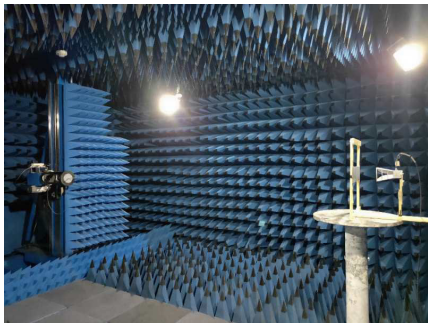

Fig. 8. Transmitarray antenna under measurement in the microwave anechoic chamber.

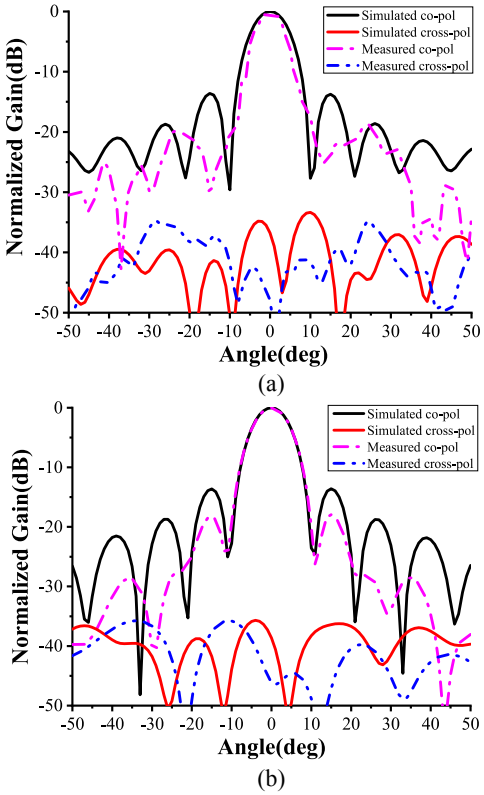

Fig. 9. The normalized measured and simulated radiation patterns at 18.5 GHz: (a) E-plane (b) H-plane.

unit cell, the dimension of the corresponding unit cell can be determined from Fig. 4.

3.2 Experimental results

The test of transmitarray antenna was carried out in the microwave anechoic chamber of Xidian University, China, as shown in Fig. 8. Fig. 9 is the measured and simulated radiation patterns of the transmitarray antenna at 18.5 GHz. As shown in the Fig. 9(a), for the E-plane pattern, the sidelobe level is 14 dB and the cross-polarization level is 34 dB. In the Fig. 9(b), for the H-plane pattern, the sidelobe level is 14 dB and the cross-polarization level is 36 dB. Fig. 10 shows the measured/simulated gains and aperture efficiency versus frequency. The measured and simulated 1-dB gain bandwidths are 14.8% (17.5–20.3 GHz) and 15.3% (17.5–20.4 GHz). The measured gain is 22.5 dBi at 18.5 GHz and the simulated gain is 22.8 dBi at 18.5 GHz. The corresponding aperture efficiency ε_{ap} is calculated using

$$\varepsilon_{ap} = \frac{G}{D_{max}} \quad D_{max} = \frac{4\pi A}{\lambda_0^2} \tag{3}$$

where G is the measured gain, D_{max} is the maximum directivity, A is the area of the transmitarray, and λ_0 is the wavelength in free-space. According to Eq. (3), we can calculate the aperture efficiency is 46% at 18.5 GHz. Because of the fabrication errors and measurement errors, the measured maximum gain is 0.3 dB lower than the simulated maximum gain. Compared to the published works in [2, 3, 4] and [19], the proposed TA has the advantages of wideband, low profile and high efficiency. Table II is a comparison of the TA performance presented in this paper with that in recent published works.

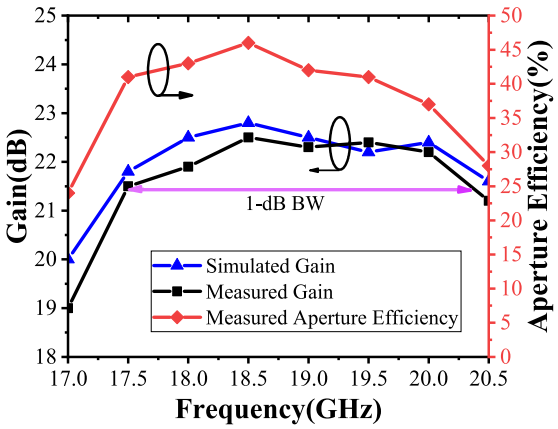

Fig. 10. Simulated/measured gains and measured aperture efficiency versus frequency.

Table II. Comparison of the proposed TA with referenced TA

Ref.	Freq. (GHz)	Aperture Efficiency (%)	Gain (dB)	1 dB Bandwidth (%)	Total thickness (mm)
[2]	12.5	20.9	18.9	9.6	0.52λ
[3]	13.58	55	23.9	7.4	0.75λ
[4]	6.1	27	20.1	8.3	0.61λ
[19]	13.5	47	29.95	11.7	0.76λ
This Work	18.5	46	22.5	14.8	0.15λ

4. Conclusion

In this paper, a wideband with low profile characteristic TA is presented. By introducing a slot-type Jerusalem cross as the middle layer of the unit cell, the designed novel combination TA can realize a reduced profile structure while maintaining wide bandwidth and high efficiency. After full-wave simulation of the TA, a 255-unit cell prototype is fabricated and measured. The measured results show that the transmitarray has 14.8% 1-dB gain bandwidth and the maximum aperture efficiency of 46%.

Acknowledgments

This work was supported by the National Natural Science Foundation of China (NSFC) under Project No. 61761032, Nature science foundation of Inner Mongolia under Contract No. 2019MS06006.

References

[1] A. H. Abdelrahman, *et al.*: "Transmitarray antenna design using cross-slot elements with no dielectric substrate," IEEE Antennas Wireless Propag. Lett. **13** (2014) 177 (DOI: 10.1109/LAWP.2014.2298851).
[2] G. Liu, *et al.*: "A high-efficiency transmitarray antenna using double split ring slot elements," IEEE Antennas Wireless Propag. Lett. **14** (2015) 1415 (DOI: 10.1109/LAWP.2015.2409474).
[3] J. Yu, *et al.*: "Design of a transmitarray using split diagonal cross elements with limited phase range," IEEE Antennas Wireless Propag. Lett. **15** (2016) 1514 (DOI: 10.1109/LAWP.2016.2517019).
[4] X. Zhong, *et al.*: "Design of multiple-polarization transmitarray antenna using rectangle ring slot elements," IEEE Antennas Wireless Propag. Lett. **15** (2016) 1803 (DOI: 10.1109/LAWP.2016.2537386).
[5] C. G. M. Ryan, *et al.*: "A wideband transmitarray using dual-resonant double square rings," IEEE Trans. Antennas Propag. **58** (2010) 1486 (DOI: 10.1109/TAP.2010.2044356).
[6] A. H. Abdelrahman, *et al.*: "High-gain and broadband transmitarray antenna using triple-layer spiral dipole elements," IEEE Antennas Wireless Propag. Lett. **13** (2014) 1288 (DOI: 10.1109/LAWP.2014.2334663).
[7] Q. Luo, *et al.*: "Wideband transmitarray with reduced profile," IEEE Antennas Wireless Propag. Lett. **17** (2018) 450 (DOI: 10.1109/LAWP.2018.2794605).
[8] X. Yi, *et al.*: "A double-layer highly efficient and wideband transmitarray antenna," IEEE Access **7** (2019) 23285 (DOI: 10.1109/ACCESS.2019.2893608).
[9] B. Rahmati and H. R. Hassani: "High-efficient wideband slot transmitarray antenna," IEEE Trans. Antennas Propag. **63** (2015) 5149 (DOI: 10.1109/TAP.2015.2476344).
[10] T. Cai, *et al.*: "High-efficiency metasurface with polarization-dependent transmission and reflection properties for both reflectarray and transmitarray," IEEE Trans. Antennas Propag. **66** (2018) 3219 (DOI: 10.1109/TAP.2018.2817285).
[11] M. A. Al-Joumayly and N. Behdad: "Wideband planar microwave lenses using sub-wavelength spatial phase shifters," IEEE Trans. Antennas Propag. **59** (2011) 4542 (DOI: 10.1109/TAP.2011.2165515).
[12] C. Tian, *et al.*: "A wideband transmitarray using triple-layer elements combined with cross slots and double square rings," IEEE Antennas Wireless Propag. Lett. **16** (2017) 1561 (DOI: 10.1109/LAWP.2017.2651027).
[13] K.-W. Lam, *et al.*: "Implementation of transmitarray antenna concept by using aperture-coupled microstrip patches," Asia-Pacific Microwave Conference (1997) 433 (DOI: 10.1109/APMC.1997.659416).
[14] H. Sun and W. Zhang: "Design of broadband element of transmit-array with polarization transform," Int. Workshop on Antenna Technology: Small and Smart Antennas, Metamaterials and Applications (2007) 287 (DOI: 10.1109/IWAT.2007.370131).
[15] L. Chang, *et al.*: "A three-layer transmitarray element with 360° phase range," IEEE International Symposium on Antennas and Propagation & USNC/URSI National Radio Science Meeting (2015) 1868 (DOI: 10.1109/APS.2015.7305323).
[16] Y. Cai, *et al.*: "A novel ultrawideband transmitarray design using tightly coupled dipole elements," IEEE Trans. Antennas Propag. **67** (2019) 242 (DOI: 10.1109/TAP.2018.2878079).
[17] W. Pan, *et al.*: "An amplifying tunable transmitarray element," IEEE Antennas Wireless Propag. Lett. **13** (2014) 702 (DOI: 10.1109/LAWP.2014.2313596).
[18] B. Rahmati and H. R. Hassani: "Low-profile slot transmitarray antenna," IEEE Antennas Wireless Propag. Lett. **63** (2015) 174 (DOI: 10.1109/TAP.2014.2368576).
[19] A. H. Abdelrahman, *et al.*: "Bandwidth improvement methods of transmitarray antennas," IEEE Trans. Antennas Propag. **63** (2015) 2946 (DOI: 10.1109/TAP.2015.2423706).
[20] M. Li and N. Behdad: "Wideband true-time-delay microwave lenses based on metallo-dielectric and all-dielectric lowpass frequency selective surfaces," IEEE Trans. Antennas Propag. **61** (2013) 4109 (DOI: 10.1109/TAP.2013.2263784).
[21] M. Li, *et al.*: "Broadband true-time-delay microwave lenses based on miniaturized element frequency selective surfaces," IEEE Trans. Antennas Propag. **61** (2013) 1166 (DOI: 10.1109/TAP.2012.2227444).
[22] M. A. Al-Joumayly and N. Behdad: "Wideband planar microwave lenses using sub-wavelength spatial phase shifters," IEEE Trans. Antennas Propag. **59** (2011) 4542 (DOI: 10.1109/TAP.2011.2165515).
[23] S. Yu, *et al.*: "One-bit digital coding broadband reflectarray based on fuzzy phase control," IEEE Antennas Wireless Propag. Lett. **16** (2017) 1524 (DOI: 10.1109/LAWP.2017.2647743).
[24] C. D. Giovampaola and N. Engheta: "Digital metamaterials," Nat. Mater. **13** (2014) 1115 (DOI: 10.1038/nmat4082).
[25] T. J. Cui, *et al.*: "Coding metamaterials, digital metamaterials and programmable metamaterials," Light Sci. Appl. **3** (2014) e218 (DOI: 10.1038/lsa.2014.99).
[26] G. Zhang, *et al.*: "A novel pattern reconfigurable wideband slot antenna using PIN diodes," International Conference on Microwave and Millimeter Wave Technology (2010) 22 (DOI: 10.1109/ICMMT.2010.5525298).
[27] R. Lian, *et al.*: "Design of a broadband polarization-reconfigurable Fabry–Perot resonator antenna," IEEE Antennas Wireless Propag. Lett. **17** (2018) 122 (DOI: 10.1109/LAWP.2017.2777502).
[28] S. Chen, *et al.*: "A multi-linear polarization reconfigurable unidirectional patch antenna," IEEE Trans. Antennas Propag. **65** (2017) 4299 (DOI: 10.1109/TAP.2017.2712185).
[29] W. Lin and H. Wong: "Polarization reconfigurable aperture-fed patch antenna and array," IEEE Access **4** (2016) 1510 (DOI: 10.1109/ACCESS.2016.2552488).
[30] A. Bhattacharjee, *et al.*: "Polarization-reconfigurable compact monopole antenna with wide effective bandwidth," IEEE Antennas Wireless Propag. Lett. **18** (2019) 1041 (DOI: 10.1109/LAWP.2019.2908661).